Towards a better understanding of bone metastatic pain: a multimodal micro-imaging approach
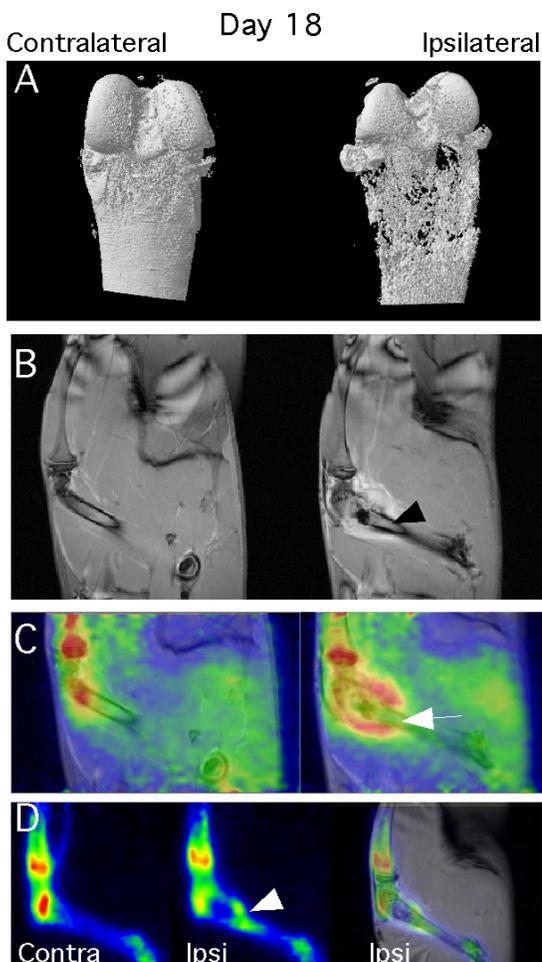
L. Dore-Savard[1,2], L. Tremblay[3,4], M. Archambault[3,4], J-F. Beaudoin[3,4], N. Beaudet[1,2], E. E. Turcotte[3,4], R. Lecomte[3,4], P. Sarret[1,2], and M. Lepage[3,4]

[1]Physiologie et biophysique, Universite de Sherbrooke, Sherbrooke, Quebec, Canada, [2]Centre des Neurosciences de Sherbrooke, Sherbrooke, Quebec, Canada, [3]Médecine nucléaire et radiobiologie, Universite de Sherbrooke, Sherbrooke, Quebec, Canada, [4]Centre d'imagerie moléculaire de Sherbrooke, Sherbrooke, Quebec, Canada

Introduction: Half of the patients suffering from cancer cannot find relief with existing analgesic treatments. Severe cancer pain is typically induced by bone metastases involving bone remodelling and nerve infiltration or compression. Non-steroidal anti-inflammatory drugs or opiates aimed at relieving inflammation and neuropathy-associated pain have undesirable side effects or are not efficient. A novel animal model of bone cancer pain to study novel treatment options is clearly needed. We have developed such a model and disgined a study to correlate the evolution of pain observed by behavioral tests during bone cancer growth with tumor-induced changes in bone content, morphology and molecular characteristics determined by µCT, MRI and PET imaging.

Day 18 — Contralateral / Ipsilateral (A, B, C, D); Contra, Ipsi, Ipsi

Methods: Bone cancer was induced by the injection of syngenic malignant mammary carcinoma MRMT-1 cells (3×10^4) in the medullar space of the femur of Sprague-Dawley rats. Behavioral indications of pain were evaluated over a 3-week period. Meanwhile, bone tumor development and structural damage to the femur were monitored by MRI using both T_2-weighted images (TR/TE$_{eff}$: 2000/12 ms, 8 echoes, FOV: 60 x 60 mm^2, matrix: $(256)^2$, NA: 8, 30 sagittal slices of 1.5 mm), T_1-weighted images (TR/TE: 320/3.3ms, FOV: 60 x 60 mm^2, matrix: $(256)^2$, α: 30°, NA: 8, 30 sagittal slices of 1.5mm, Gd-DTPA) and PET (Na^{18}F: 10MBq, 30 min acquisition, 30 min after injection or [^{11}C]methionine: 74MBq, 30 min acquisition, 30 min after injection) at day 0, 8, 10, 13 (MRI only), 15, 18 and 21 following cancer cells inoculation. PET scans were performed immediately following MRI acquisitions while the animal remained under anaesthesia in a custom-made hind limbs positioning device. Images could thus be superimposed to facilitate interpretation. At different times following behavioral tests, whole femurs were extracted post-mortem and imaged with a µCT scanner (source: 80 kV, 124 µA; zoom: 20X; pixel size: 14 µm; exposition time: 3.0 s; rotation: 0.9°).

Results: At day 14 post-surgery, a significant reduction in the response threshold of hind paw withdrawal to von Frey allodynic stimulations and a decreased weight bearing on the affected limb were detected. Accordingly, MR images showed progressive damage to the bone environment from day 10 post-inoculation. It is noteworthy that the tumour was consistently detected before pain behavior was observable. Indeed, the tumor was readily detectable in the MR images by a relative increase in voxel intensities in the inoculated region. Evidence of tumor development was subsequently observed with PET and correlates exactly with MR in the co-registered images (Fig. 1B, C, D). Moreover, Na^{18}F distribution was highly modified compared to the contralateral hind limb in the tumor bearing bone (Fig 1D, white arrowhead). High ^{18}F$^-$ concentration in tumour surrounding areas is presumably indicative of osteoblastic compensative bone formation, a direct consequence of the lytic properties of the tumour. The latter is supported by µCT analysis (Fig. 1A). In fact, both the bone volume/tissue volume ratio and the trabecular pattern factor (an indicator of bone connectiveness) are modified in tumor bearing bones. Additionally, [^{11}C]methionine uptake, indicative of protein synthesis, was highly specific to the tumor, especially in bone emerging areas of the bone tumor (Fig. 1C, white arrow). However, this tracer does not accumulate in the proximal medullar channel as expected considering the high intensity observed in both T_1- and T_2-weighted images (Fig 1B, black arrowhead). This observation is of significant interest for the discrimination between tumor and inflammation.

Conclusion: MRI-PET co-registration and µCT were used to characterize tumor metabolism and growth in a novel model of bone cancer pain. The complementary information provided by this multimodality imaging enables a more complete evaluation of the different components playing a role in bone cancer pain. This approach will help understanding better the mechanisms underlying genesis and maintenance of bone cancer pain *in vivo*, which will be useful in the development of new and improved analgesic treatments.